Journal of Nuclear Materials 405 (2010) 165–170

Contents lists available at ScienceDirect

Journal of Nuclear Materials

journal homepage: www.elsevier.com/locate/jnucmat

Strengthening effect of Cr_2O_3 thermally grown on alloy 617 foils at high temperature

S.K. Sharma [a,b], F.X. Li [a], G.D. Ko [a], K.J. Kang [a,*]

[a] Department of Mechanical Engineering, Chonnam National University, 300-Youngbong dong, Buk-gu, Gwangju 500 757, Republic of Korea
[b] MINT, Dongguk University, Jung-gu, Seoul 100715, Republic of Korea

ARTICLE INFO

Article history:
Received 18 August 2009
Accepted 9 August 2010

ABSTRACT

Alloy 617 has been selected for the intermediate heat exchanger (IHX) of the very high temperature gas-cooled reactor (VHTR) for the economic production of electricity and hydrogen. In this work, the strengthening effects of Cr_2O_3 thermally grown on alloy 617 foils at 800 and 900 °C were investigated. A micro-tensile test system was used for *in situ* measurement of tensile strain in the foils and superficial thermally-grown Cr_2O_3. Each foil was heated until the thermally-grown Cr_2O_3 reached a predetermined thickness; then, a load was applied to measure the tensile response. As the Cr_2O_3 layer thickened on the surface of the metal foils, the strengths and stiffnesses of the foils were enhanced. We assumed that there was no interaction between the substrate and the superficial chromia, and the strength of Cr_2O_3 itself was measured. At 800 °C, the Cr_2O_3 was brittle and the strength was governed by crack initiation. At 900 °C, the Cr_2O_3 was much more ductile, and strain hardening was observed for even the smallest thickness. The strength was maintained even after crack initiation was observed on the surface.

1. Introduction

The service life of metallic components used at high temperatures often depends on the formation of thin protective superficial oxide scales. Failure in producing chemically- and thermo-mechanically stable oxide scales leads to severe degradation of metallic components under service conditions. Some stable oxides such as α-Al_2O_3 and Cr_2O_3 are known to possess good mechanical properties and corrosion protection at high temperatures [1–4]. A thin, continuous scale of adherent, slow-growing alumina and/or chromia provides an effective diffusion barrier which protects the underlying alloy from deleterious oxidation [5–12]. For this reason, alloy 617 has been selected for the intermediate heat exchanger (IHX) of the very high temperature gas-cooled reactor (VHTR) for the economic production of electricity and hydrogen [13–22]. Oxidation tests of alloy 617 have demonstrated that the Cr-contained superalloys usually develop chromium-rich dense surface oxide scales and internally discrete α-Al_2O_3 in "balanced" VHTR environments [19,23–29]. However, above a critical temperature T_C ($T_C > \sim 900$ °C), the oxide scale suffers from a destructive reaction and cannot provide any protection against further corrosion. The Cr-rich oxide scale growth kinetics of bare alloy 617 obeys a parabolic rate law during the entire oxidation test [27,29].

The mechanical properties of the thermally-grown oxides (TGOs) which form on heat-resistant alloys are essential considerations for structural design and corrosion protection at high temperatures. It is expected that the Cr-rich oxide scale has a beneficial effect on the tensile strength of alloy 617 components, as observed in Fecralloy foil specimens [30]. Wright [25] investigated the role of oxide layers on the tensile properties of a standard specimen (cylindrical type) of alloy 617. They observed that the yield strength at room temperature decreased as exposure time increased at 1000 °C. The main objective of this work is to investigate the strengthening effect of thermally-grown Cr_2O_3 on the tensile properties of 100 μm-thick foils of alloy 617 at 800 and 900 °C. Initially, tensile properties of stand-alone alloy 617 foils were measured at 800 and 900 °C in an Argon environment. Then, the foils were exposed in air for oxidation until thermally-grown Cr_2O_3 of a predetermined thicknesses formed on the surfaces. The tensile properties of the metal foils with thermally-grown Cr_2O_3 on their surfaces were measured at the same temperatures. The microstructures of the oxides and the metal substrates were observed under a scanning electron microscope (SEM) combined with energy dispersive X-ray (EDX) mapping. We assumed that no interaction between the TGO and metal occurred, and the tensile strength of thermally-grown Cr_2O_3 was calculated.

2. Experimental: material preparation and the micro-tensile test system

Tensile tests were performed with foil specimens of commercially available Ni-based alloy 617. Details of the chemical

* Corresponding author. Tel.: +82 62 530 1668; fax: +82 62 530 1689.
E-mail address: kjkang@chonnam.ac.kr (K.J. Kang).

0022-3115/$ - see front matter
doi:10.1016/j.jnucmat.2010.08.008

composition of alloy 617 and the preparation of the foils are given in our earlier publications [29,31]. The specimens of alloy 617 were cold-rolled foils with a thickness of ~100 μm. The cold-rolled foils were annealed in a vacuum at 950 °C for 17 h and furnace-cooled at a rate of 5 °C/min. The foils were cut into ribbons with lateral dimensions of 5 × 50 mm^2 and the gage section of the tensile specimens (~3 × 15 mm^2) were prepared for the tests. Thereafter, they were mechanically ground and polished to a 1 μm finish. Prior to testing, each specimen was cleaned in acetone, and its dimensions and weight measured with accuracies of ±10 μm and ±10 μg, respectively.

Fig. 1 shows a schematic illustration of the micro-tensile test system used for the experiments. The loading actuator is a stepping motor capable of controlling the displacement with a resolution of 0.05 μm. A charge-coupled device (CCD) camera with a zoom lens was placed in front of the test rig to obtain a series of digital images of the specimen. Two infrared pyrometers, each having different wavelengths, were installed in the rear of the test rig to measure the thermally-grown Cr_2O_3 thicknesses by the emissivity difference method and temperature *in situ* [32]. Specific details of the micro-tensile test system and its specifications are given in [30]. Fig. 2 shows the configuration of the tensile specimens and the heated foil (heated via electricity passed through the specimen in a test rig). Before the tensile tests, alumina powder (particle size: 0.05 μm) and water mixture was sprayed on each specimen's gage section and dried for 2 h at 100 °C in an electric oven. This resulted in clear random dots on the surface of the gage section of the tensile specimen, thereby enabling strain mapping of the images taken during the test. The dots served as a speckle pattern which was used to measure the displacement (tensile strain) using the digital image correlation (DIC) technique [30]. The specimens were oxidized at 800 and 900 °C in air within the test system as they were subjected to a minimum load (P_{min} ~ 0.1 N). To observe the microstructures (i.e., the TGO thickness, chemical composition of the oxides, and the penetration depth of internal oxide), the foils were cut normal to the surface, polished with SiC grit papers followed by a 1 μm diamond suspension, and cleaned ultrasonically in acetone.

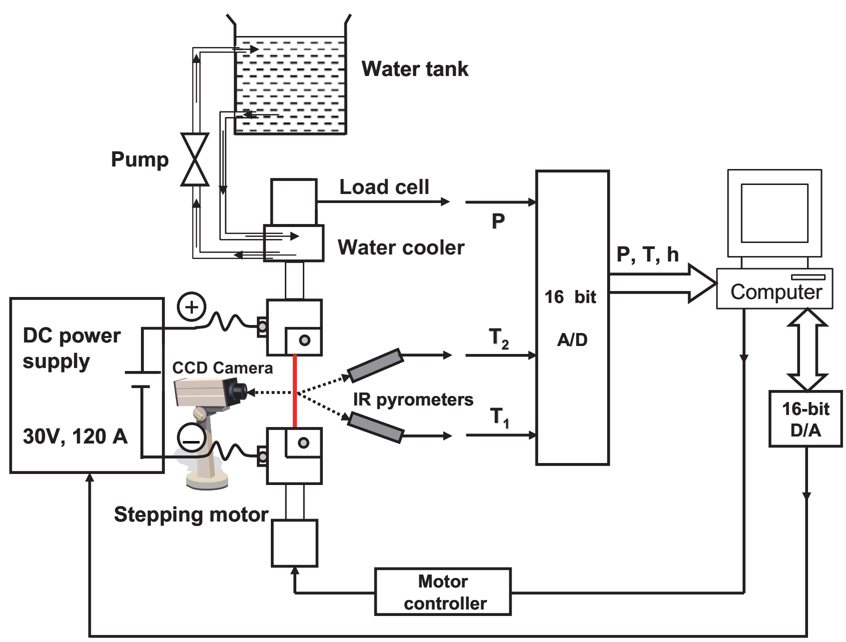

Fig. 1. Schematic illustration of the micro-tensile test system.

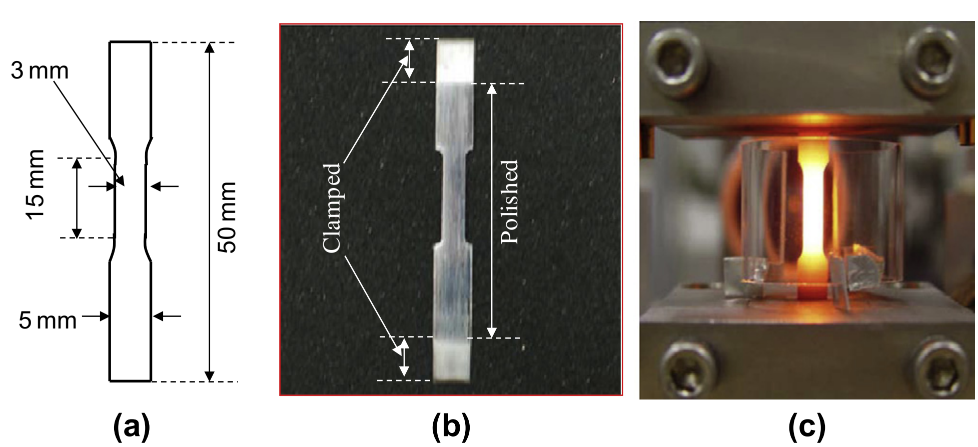

Fig. 2. Configurations of the specimen foils: (a) schematic illustration of the dimension of the foil, (b) a polished foil, and (c) photo of heated foil in the test rig.

3. Results and discussion

Fig. 3a–d shows SEM images of the cross sections of the oxidized foils of alloy 617 at 800 and 900 °C for 8 h and 48 h, respectively. The formation of surface oxides and the penetration depths of internal oxide increased as the oxidation time increased at both oxidation temperatures. To obtain the composition near the oxides, energy dispersive X-ray (EDX) mapping was used. According to the EDX mapping analysis, the uniform surface oxide scale was identified as chromia (Cr_2O_3), and the discrete internal oxide was alumina (α-Al_2O_3) [29]. For a single value of chromia TGO thickness, fifty measurements were carried per a SEM image of the cross section, and averaged. The standard deviations were almost constant in a range of 0.3–0.35. The variation of average chromia thickness versus oxidation time is shown in Fig. 4. The chromia thickness increased with oxidation time. At 800 °C, the TGO thickness increased from 0.10 to 1.10 μm as the oxidation time increased from 1 h to 72 h, whereas at 900 °C, the TGO thickness increased from 0.70 to 3.10 μm as the oxidation time increased from 1 to 72 h.

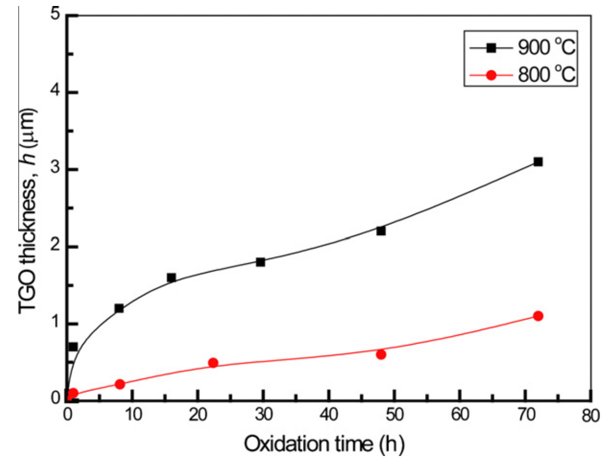

Fig. 4. Variation of the thicknesses of TGO formed on the foils of alloy 617 with respect to oxidation time at 800 and 900 °C.

Fig. 5a and b shows the stress–strain curves of the rolled-annealed foils of alloy 617 with thicknesses of thermally-grown chromia on the surfaces at 800 and 900 °C, respectively. The tensile properties of the metal foil with zero thickness of chromia were measured at 800 and 900 °C in an Argon gas environment. For the tensile tests of the metal foils with chromia on the surfaces, each foil specimen was exposed for oxidation in the test rig at the previously mentioned temperatures until the chromia TGO reached a pre-specified thickness. Thereafter, load was applied to measure the tensile strain. The thickness of metal substrate of each specimen, *H*, was measured again with accuracy of 1 μm by microscopic observation for the polished cross sections, after the oxidation and tensile test. In the figures, regardless of the test temperatures, the stress–strain curves always go upward as the

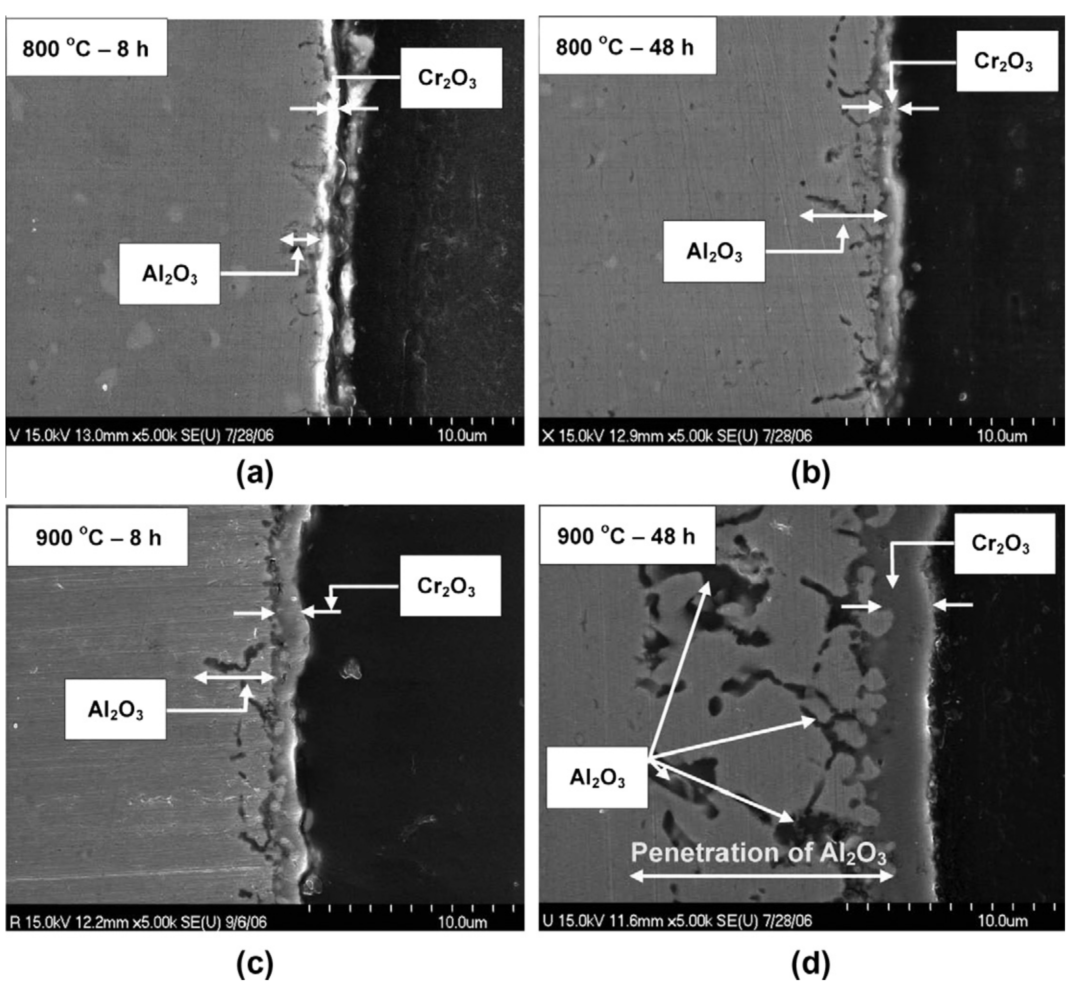

Fig. 3. Typical scanning electron microscopic (SEM) images of cross sections near the surface of the oxidized foils of alloy 617 in air at (a) 800 °C for 8 h, (b) 800 °C for 48 h, (c) 900 °C for 8 h, and (d) 900 °C for 48 h.

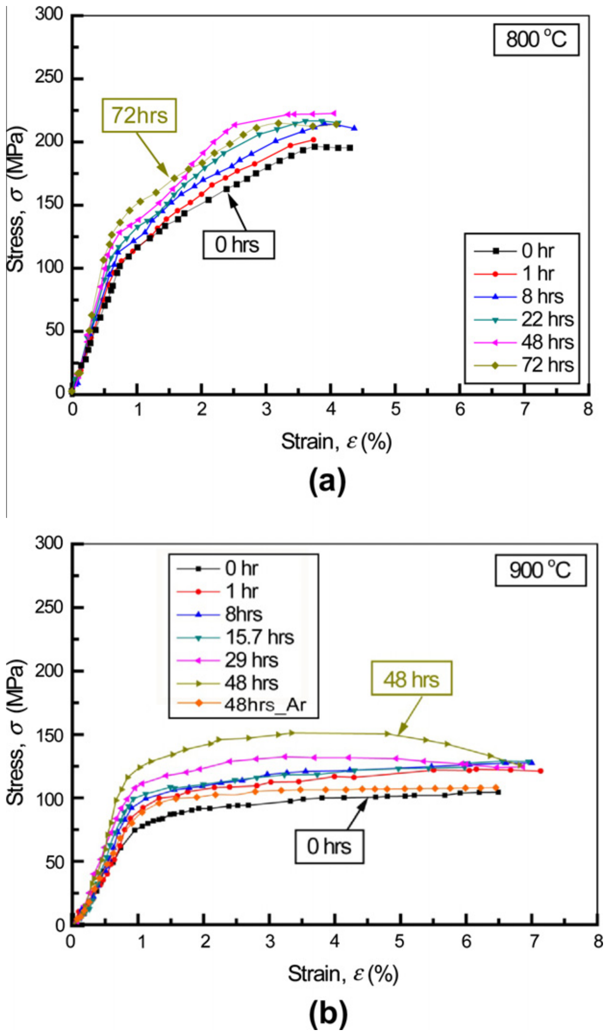

Fig. 5. Stress–strain curves of alloy 617 foils with various thicknesses of Cr_2O_3 thermally grown in air at (a) 800 °C and (b) 900 °C.

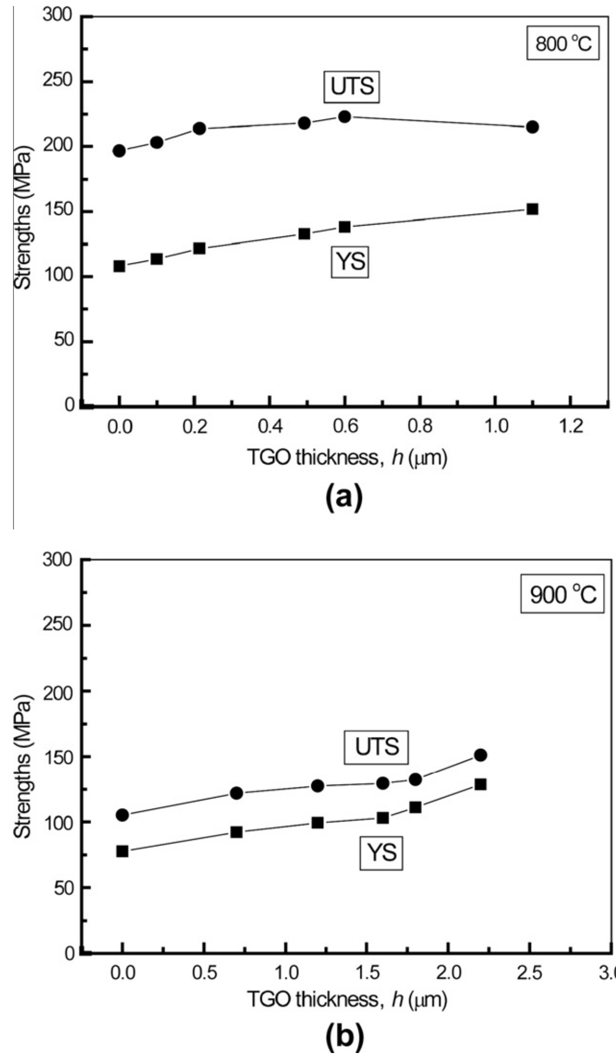

Fig. 6. Variation of yield strengths (YS) and ultimate tensile strengths (UTS) with respect to TGO thicknesses formed on foils of alloy 617 at (a) 800 °C and (b) 900 °C.

oxidation time increased, which clearly shows the strengthening effect of the chromia formed on the alloy 617. In order to check a possibility that the aging of the substrate exposed long time at the high temperature even without oxidation influenced the strength, an independent specimen was aged for 48 h at 900 °C in Argon environment, and tested to measure the tensile stress–strain curve. The result was also included in Fig. 5b. Compared with non-aged virgin specimen, the aged specimen revealed a little hardening in the strength. However, SEM observation on the cross section of the surface revealed the chromia with thickness of 0.4–0.5 μm, which seems to be due to slightest content of oxygen remaining in the environmental chamber. Therefore, it is concluded that the aging induced negligible effect on the strength of the substrate alloy because the specimens were fully annealed at the higher temperature of 950 °C for 17 h before they were tested.

To characterize the strengthening effect, the variations of yield strength (YS) and ultimate tensile strength (UTS) at 800 and 900 °C with chromia thickness are shown in Fig. 6a and b, respectively. At 800 °C, the YS increased from 113.46 to 151.84 MPa and the UTS increased from 201.78 to 226.96 MPa as the TGO thicknesses increased from 0.10 to 1.10 μm. At 900 °C, the YS increased from 92.22 to 128.61 MPa and the UTS increased from 121.82 to 159.41 MPa as the TGO thicknesses increased from 0.70 to 2.20 μm. The increased strength of alloy 617 foils with thermally-grown Cr_2O_3 indicated that the uniform TGO on the surfaces resulted in metal strengthening at the elevated temperatures.

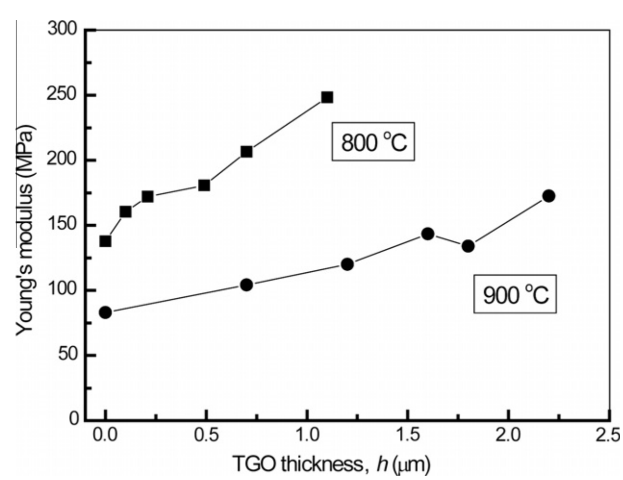

Fig. 7. Variation of Young's modulus with respect to TGO thicknesses formed on foils of alloy 617 at 800 and 900 °C.

Fig. 7 shows the variation of Young's modulus with respect to chromia TGO thicknesses at 800 and 900 °C. At 800 °C, Young's modulus increased from 130 to 250 MPa as the TGO thickness increased from 0 to 1.10 μm. At 900 °C, Young's modulus increased from 80 to 175 MPa as the TGO thickness increased from 0 to 2.2 μm. As shown in Figs. 6 and 7, the chromia TGO formed on the surfaces enhanced not only the strengths but also the stiffnesses of the foil specimens.

Assuming no interaction between the substrate and the superficial chromia TGO, the stress acting on the TGO layer, σ_{TGO}, was calculated for a tensile specimen as follows:

$$\sigma_{TGO} = \frac{F - \sigma_{Metal} \times H \times W}{2 \times h \times W} \quad (1)$$

where F is the total applied force; σ_{Metal} is the stress acting on the metal substrate, which was assumed to be the same as that measured in an inert gas (dry Ar gas) environment; H is the thickness of the substrate; h is the TGO thickness; and W is the specimen width at the gage section. Eq. (1) means that the stress acting on the TGO is calculated by subtracting the contribution of the stress acting on the substrate metal from the total force. Fig. 8a and b shows the stress–strain (σ_{TGO}–ε) curves of thermally-grown Cr_2O_3 at 800 and 900 °C, respectively. The maximum stress of thermally-grown Cr_2O_3 was observed to range from 4 to 5 GPa at 800 °C as the Cr_2O_3 thickness increased from 0.3 to 1.1 μm. At 900 °C, distinct yield points were observed and varied from 1.2 to 1.8 GPa as the thickness increased from h = 0.7 to 2.2 μm. At 800 °C, comparing the load-time data with the images taken by the CCD camera, the moment at which the stress started to drop rapidly corresponded to crack initiation on the specimen's surface. That is, the maximum stresses were governed by the crack initiation in the thermally-grown Cr_2O_3. On the contrary, at 900 °C, after some decrease following the yield points, the stress level maintained up to 4.5% strain, and strain hardening was observed for h = 0.7 μm. We conclude that at 800 °C, thermally-grown Cr_2O_3 can provide excellent mechanical protection with deformation tolerated up to only 0.5% strain. At 900 °C, the protection decreased significantly with considerably more deformation tolerated – up to ~4.5% strain – even after cracks were initiated.

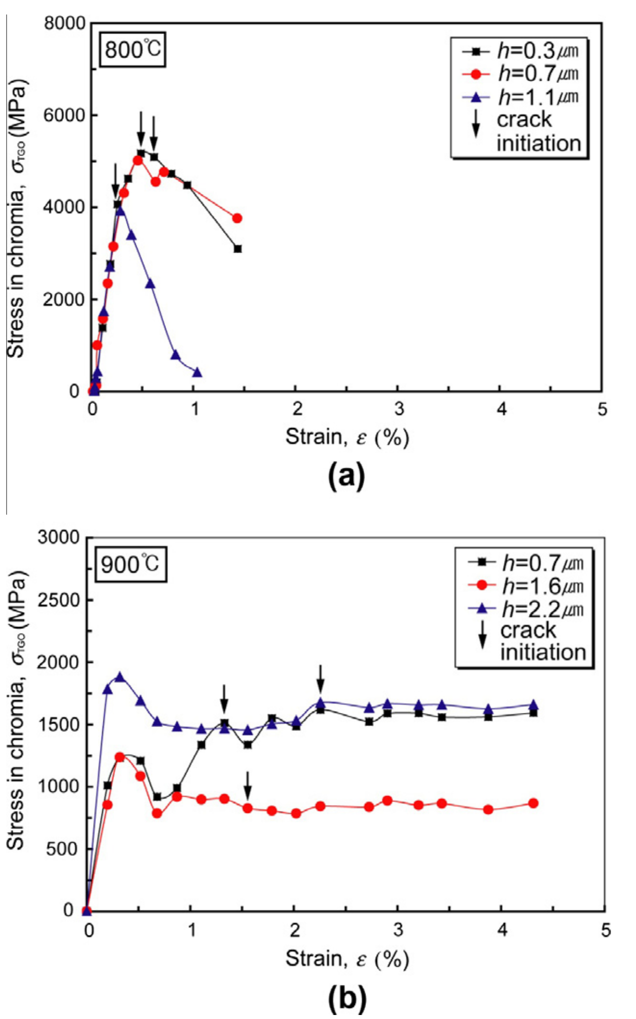

Fig. 8. Stress–strain curves of thermally-grown Cr_2O_3 with various thicknesses at (a) 800 °C and (b) 900 °C.

4. Conclusion

The strengthening effects of Cr_2O_3 thermally grown on alloy 617 foils were investigated at 800 and 900 °C. The strengths and stiffness of the metal foils were enhanced with the chromia formed on the surface, which indicated that the surface oxide played an important role in the durability of the alloy at elevated temperatures. Assuming no interaction between the substrate and the superficial chromia TGO, at 800 °C, the maximum stress of the chromia was observed to vary from 4 to 5 GPa as the thickness increased from 0.3 to 1.1 μm, while at 900 °C, the yield point was clearly observed and varied from 1.2 to 1.8 GPa as the thickness increased from 0.7 to 2.2 μm. However, at 800 °C, the Cr_2O_3 was brittle and the strength was governed by crack initiation, while at 900 °C the Cr_2O_3 was much more ductile and maintained its strength, and even strain hardening was observed for the Cr_2O_3 with the smallest thickness. We conclude that at 800 °C, thermally-grown Cr_2O_3 can provide excellent mechanical protection with deformation tolerated up to only 0.5% strain, while at 900 °C the protection decreases significantly, with much more deformation tolerated up to ~4.5% strain even after cracks are initiated.

Acknowledgements

This work was performed under a program of the Basic Atomic Energy Research Institute (BAERI), which is a part of the Nuclear R&D Programs of the Ministry of Science & Technology (MOST), and one of the authors, S.K. Sharma, was financially supported by the BK-21 program, Republic of Korea. The authors would like to thank Dr. J.W. Choi, POSCO, Korea for rolling the foils.

References

[1] C.H. Shek, K.W. Wong, J.K.L. Lai, Mater. Sci. Eng. (R) 19 (1997) 153–200.
[2] E. Kroke, Y.L. Li, C. Konetschny, E. Lecomete, C. Fasal, R. Riedel, Mater. Sci. Eng. (R) 26 (2000) 97–199.
[3] M. Schutze, Protective Oxide Scale and their Breakdown, John Wiley & Sons, England, 1997.
[4] A.G. Evans, D.R. Mumm, J.W. Hutchinson, G.H. Meier, F.S. Pettit, Prog. Mater. Sci. 46 (2001) 505–553.
[5] L. Tan, K. Sridharan, T.R. Allen, J. Nucl. Mater. 371 (2007) 171.
[6] P.S. Shankar, K. Natesan, J. Nucl. Mater. 366 (2007) 28.
[7] N. Birks, G.H. Meier, F.S. Pettit, Introduction to the High Temperature Oxidation of Metals, Cambridge University Press, 2006 [Chapter 5].
[8] H.J. Grabke, Surf. Interface Anal. 30 (2000) 112–119.
[9] R. Cueff, H. Buscail, E. Caudron, F. Riffard, C. Issartel, S.E. Messki, Appl. Surf. Sci. 229 (2004) 233–241.
[10] D.R. Clarke, Acta Mater. 51 (2003) 1391–1407.
[11] V.K. Tolpygo, D.R. Clarke, Surf. Coat. Technol. 120–121 (1999) 1–7.
[12] V.K. Tolpygo, D.R. Clarke, Acta Mater. 47 (1999) 3589–3605.
[13] J.A. Lake, Foundations for the Forth Generation of Nuclear Reactor, Nuclear News, November 2000, p. 32.
[14] D.J. Hill, Back to the future: nuclear energy research at ORNL, Review 37 (2004) 1–32.
[15] T. Angeliu, J. Ward, J. Witter, Assessing the Effects of Radiation Damage on Ni-base Alloys for the Prometheus Space Reactor System, LM-06K033, P.O. Box 1072, Schnecetady, New York, USA, April 2006.

[16] F. Rouillard, C. Cabet, K. Wolski, A. Terlain, M. Tabarant, M. Pijolat, F. Valdivieso, J. Nucl. Mater. 362 (2007) 248.
[17] F.M. Olbersleben, N. Kasik, B. Ilschner, F.R. Aria, Metall. Mater. Trans. A 30 (1999) 981.
[18] J. Chen, T. Muroga, T. Nagasaka, Y. Xu, S. Qiu, J. Nucl. Mater. 322 (2003) 73–79.
[19] A. Kewther, B.S. Yilbas, M.S.J. Hashmi, J. Mater. Eng. Perform. 10 (2001) 108.
[20] M.A. Kewther, B.S. Yilbas, M.S.J. Hashmi, Indust. Lub. Tribol. 53 (2001) 112.
[21] M.K. Ali, M.S.J. Hashmi, B.S. Yilbas, J. Mater. Process. Technol. 118 (2001) 45.
[22] D. Allen, J.P. Keustermans, S. Gijbels, V. Bicego, Mater. High Temp. 21 (2004) 55.
[23] T. Hirano, M. Okada, H. Araki, T. Noda, H. Yoshida, R. Watanabe, Metallurg. Trans. A 12 (1981) 451–458.
[24] H.J. Christ, U. Kunecke, K. Meyer, H.G. Sockel, Mater. Sci. Eng. 87 (1987) 161–168.
[25] R.N. Wright, Summary of Studies of Aging and Environment effect on Inconel 617 and Hayans 230, Idaho National Laboratory, INL/EXT-0611750, 2006.
[26] F. Rouillard, C. Cabet, K. Wolski, A. Terlain, M. Tabarant, M. Pijolat, F. Valdivieso, J. Nucl. Mater. 362 (2007) 248–252.
[27] C. Jang, D.J. Lee, D.J. Kim, Int. J. Press Vessels Piping 85 (2008) 368–377.
[28] F. Rouillard, C. Cabet, K. Wolski, M. Pijolat, Oxid. Met. 68 (2007) 133–148.
[29] S.K. Sharma, G.D. Ko, F.X. Li, K.J. Kang, J. Nucl. Mater. 378 (2008) 144–152.
[30] S.K. Sharma, G.D. Ko, K.J. Kang, J. Euro. Ceram. Soc. 29 (2009) 355–362.
[31] S.K. Sharma, C. Jang, K.J. Kang, J. Nucl. Mater. 389 (2009) 420–426.
[32] S.S. Lee, S.K. Sun, K.J. Kang, Oxid. Met. 63 (2005) 73–85.